https://doi.org/ 10.48048/tis.2022.5602

Strengthened of a Square RC Columns using BFRP and GFRP: The Experimental Investigations

Tejash Patel*, Sanjay Salla, Sandip Vasanwala and Chetankumar Modhera

Department of Civil Engineering, Sardar Vallabhbhai National Institute of Technology, Gujarat 395007, India

(*Corresponding author's e-mail: er.tejashpatel@gmail.com)

Received: 11 December 2021, Revised: 9 March 2022, Accepted: 8 April 2022

Abstract

Reinforced concrete (RC) columns, jacketing of FRPs has become a standard strengthened technique in the present times. The current research scenario focuses on the fact that strengthened and rehabilitation of RC columns by CFRP and GFRP are more effective. Additionally, the present research also highlights a new class of natural composites of BFRP (Basalt Fiber Reinforced Polymer) bonded with adhesive to column specimens as an alternate confinement material. Generally, it is advisable to use RC columns instead of CFRP and GFRP confinement material. The experimental study was strengthened by partially and fully wrapped square RC columns using GFRP and BFRP uni - directional and bi-directional. The behavior of stress-strain curves and failure modes were observed. The experimental results show that the substantial increment in ultimate load-displacement capacity, ultimate stress-ultimate axial and lateral strains lead to BFRP and GFRP failure. The fully warped square reinforced concrete (RC) column performs better in getting stress-strain behavior and displacement limit as compared to the partially covered system. It is a fact that the strengthened obtained by partial wrapping with BFRP and GFRP is a preferable and cost-effective alternative as compared to the fully wrapped. The test results show that the CNR-DT-R1 model is more reliable than Lam & Tang and provides reasonable and precise calculations for the ultimate axial stress of partially and fully wrapped RC columns.

Keywords: Square columns, BFRP and GFRP, Partial strengthening, Full strengthening, Stress-strain behavior

Introduction

Reinforced concrete (RC) is the predominantly traditional building material being used all over the world. All structural members of older building structures designed from previous design codes have been weakened in strength and ductility of concrete due to natural disasters like earthquakes, tsunamis, fires, cyclones, floods, durability aspects, and the periodic time interval. Moreover, there is an increment in load due to changes in its usage. It was not rare to find that some structural members could be deteriorated or even damaged in this way. This deterioration or damaged structural member should be repaired, rehabilitated, or restored as per the structural member's requirement and condition. The utilization of fiber -reinforced polymer (FRP) is very convenient for the strengthened of the structural member. FRP material has excellent properties, strength, less stiffness, cost-effectiveness, ductility, and corrosion resistance. The use of FRP enhances the compressive ductility and strength of the RC columns [1-5]. The extensive experimental studies demonstrate that the strengthened of RC column specimens shows the load-displacement capacity. It is governed by the significant influential parameters like the compressive strength, cross-section area, aspect ratio of the column specimens, different radius, the number of wrap layers, the orientation of FRP wrap, ratio and orientation of longitudinal reinforcement, and the nature of loading [6-11]. The performance of fully FRP wrapped columns were investigated by many researchers [12,13]. The behavior of cylinders and prisms on partially FRP wrapped [14-16], and reinforced concrete columns [17-19] have been attempted by a few researchers. The corner radius of samples examined by Saljoughian and Mostofinejad was 8 m^2 [14,15] which is substantially less than the suggested corner radius in ACI 440.2 R-17 [16] of 13 m^2 and FIB bulletin 14 of 20 m^2 [17]. The behavior of partly FRP-covered concrete cylinders was experimentally studied with fully FRP-wrapped concrete

cylinders under axial compression. According to the experimental observations, the compressive strength of partially wrapped concrete cylinders is less than the compressive strength of entirely covered concrete cylinders [14,16,23]. Partial wrapping of concrete cylinders also led to increasing compressive strength and axial deformation compared to non-wrapped specimens [14,16].

Partly covered FRP square RC columns should be widely calculated and matched to the behavior of entirely covered FRP square RC columns to understand the strength and ductility enhancement of partial wrapping. carbon, aramid, and glass are the most popular fiber types the among others utilized materials [18-20]. Basalt fibers have also been used more recently. By melting basaltic rock and afterwards spinning the molten substance, basalt fibers are obtained. The new manufacturing expertise for continuous basalt fibers is very comparable to that used to manufacture E-glass.

Simultaneously, basalt filament is made by melting the basalt rock without any other additives and it benefits to the optimization of the cost. In this, lower energy is required due to the ease of the manufacturing procedure [21]. This research aims at comparing the experimental results of different external strengthened configurations such as basalt fiber and glass fibers. In terms of structural performance, the strengthened evaluation described here focuses more on the axial stress-strain behavior of square RC columns by applying full and partial GFRP and BFRP strengthened techniques. This study aims to determine the efficiency of the FRP reinforcement technique from an economic perspective. Various results were obtained, such as ultimate load, displacements and axial stress in the concrete, whereas ultimate lateral strain in FRP wrapping. Additionally, the study has been performed to verify the experimental data's reliability and accuracy with the theoretical models such as CNR-DT R1 [22] Lam & Teng model [23].

Experimental programme

Details of column specimens

In the present study, the effect of partial strengthened and full strengthened of an axially loaded short RC column by using GFRP and BFRP material with uni-directional and bi-directional wrapping respectively, is evaluated. The different strengthened columns were prepared along with the non-strengthened columns, details, as shown in **Table 1**.

All square RC columns were designed based on IS-456-2000 [24]. The square column cross-section dimensions were 170 m^2×170 m^2 and height of 700 m^2, as shown in **Figure 1**.

Table 1 RC column strengthening details.

Sr. No.	Specimen ID	Type of Strengthening	Specimen details		
			B (m^2)	D (m^2)	L (m^2)
1	**S 1**	Non-strengthened	170	170	700
2	**B1X**	Top strengthened (Series-I)	170	170	700
3	**G1X**		170	170	700
4	**B2X**		170	170	700
5	**G2X**		170	170	700
6	**B1Y**	Top-Bottom strengthened (Series-II)	170	170	700
7	**G1Y**		170	170	700
8	**B2Y**		170	170	700
9	**G2Y**		170	170	700
10	**B1Z**	Full strengthened (Series-III)	170	170	700
11	**G1Z**		170	170	700
12	**B2Z**		170	170	700
13	**G2Z**		170	170	700

*G = Glass fiber, B = Basalt fiber, 1 = Unidirectional of material, 2 = Bidirectional of material, X = Top strengthening, Y= Top-Bottom strengthening and Z= Full strengthening.

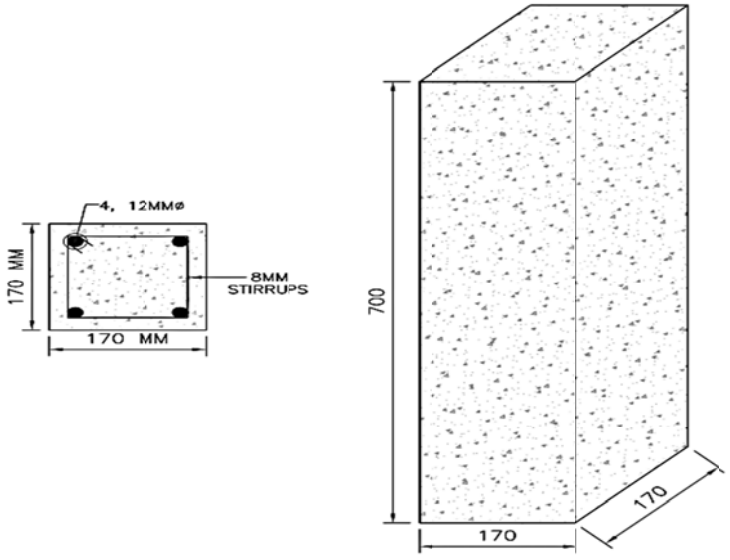

Figure 1 Reinforcement detail of square column.

Material properties

Reinforcement bar

In this study, the locally available reinforcement bars of grade Fe-500 are used. The ultimate tensile strength of 12 and 8 m^2 bar was obtained as 587 and 576 N/m^2, respectively. The percentage elongation was 21.66 and 29.25 %, respectively as per IS1786: 2008 [25].

Concrete

The mix design of the M25 grade of concrete was prepared as per IS 10262:2009 [26]. **Table 2** exhibits the relative proportion of concrete constituents. The average compressive strength of concrete was obtained 31.23 MPa.

Table 2 Concrete Mix design.

Cement (kg/m^3)	FA (Sand) (kg/m^3)	CA (20 m^2) (kg/m^3)	CA (10 m^2) (kg/m^3)	Water (kg/m^3)
340	961	692	446	168

FRP wraps and epoxy resin

The flat coupon tensile test has been carried out to determine the properties of GFRP and BFRP wraps. **Figure 2** shows the uni-directional and bidirectional 1-layer flat coupons. The test method was followed by the recommendations specified in the ASTM-D3039: 2008 [27]. A total of 5 flat coupons of each FRP were tested, and the elastic modulus of the tensile strength and the mean values of the rupture stress were determined, as shown in **Table 3**.

Figure 2 Tensile test of different FRPs.

Table 3 Different Properties of FRPs and resin.

FRP wraps	BFRP Unidirectional	GFRP Unidirectional	BFRP Bidirectional	GFRP Bidirectional	Adhesive
Thickness (m^2)	0.115	0.36	0.32	0.66	-
Tensile strength (MPa)	2100	2400	1950	2785	30
E-Modulus (GPa)	105	72	93	73	4500
Elongation (%)	2.6	2.3	2.3	1.96	1.5

Partially and fully strengthening of column elements

The RC column specimens strengthened was carried out as per ACI 440.2R-2017 [16]. A smooth curvature at the corner of square columns was provided at a radius of 20 m^2 to get stronger confinement of columns, as shown in **Figure 3**. The wet lay-up technique was implemented to strengthen the column. The specimen's concrete surface was impregnated with the adhesive before placing the GFRP, and BFRP wraps to strengthen the GFRP and BFRP wraps' specimens. GFRP and BFRP wraps were situated in the uni-direction and bi-directional in partial and full manner. As shown in **Figure 3**, the specimens confined with single layers were enclosed with overlap based on ACI-440-2R-2017 [16].

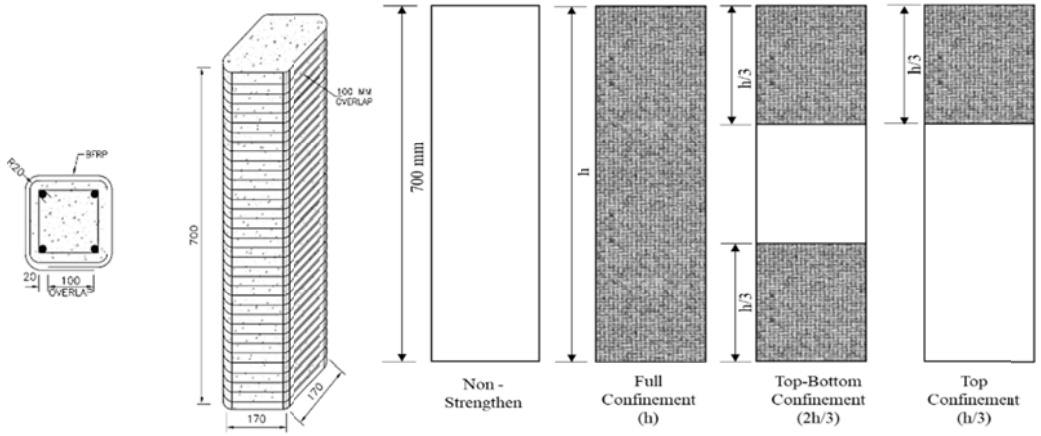

Figure 3 Column strengthening details.

Testing procedure

The details of the test setup and instrumentation of RC column to measure the axial compression are elaborately discussed in this section. There were the LVDTs, strain gauges, and load cells instrumented at the columns testing. Initially, the column was loaded up to 10 kN. Three charging and discharge cycles for 10 kN of its planned peak load were carried out to ensure that the surface undulation was eliminated from the reinforced concrete column components. It was observed that the pure axial load was protected by up to 10 - 15 kN of the applying load. As the column remained under compression during the test, the instrument was organized for the concentrated axially. The strain gages are placed on the column's surface to measure the strains in the longitudinal and transverse directions, as shown in **Figure 4**. All the data for load, displacement and strain measurements of concrete and FRP material were obtained by using the Data Acquisition System (DAQ).

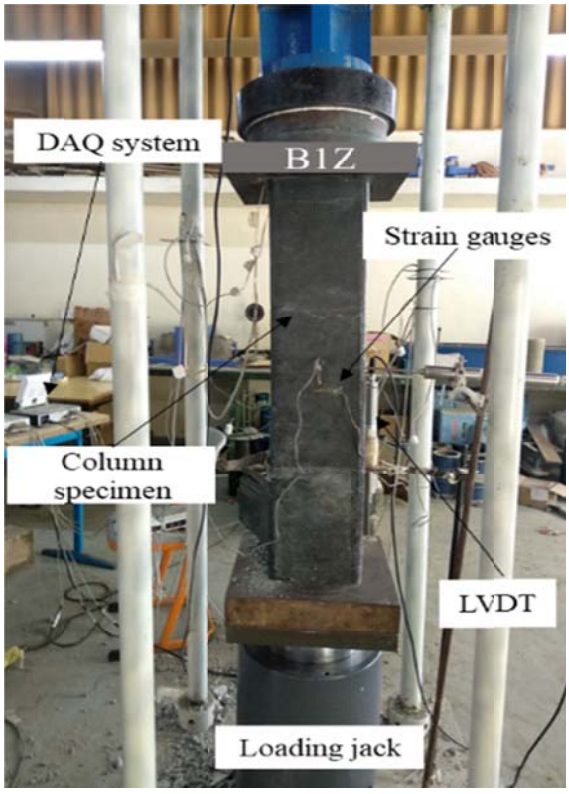

Figure 4 Test set up and instruments.

Results and discussion

Failure modes

The non-strengthen and strengthened RC square column elements were tested until they reached to their ultimate load. In the non-strengthen RC column specimens, vertical line-like cracks appear from the middle part to the top part of the square column, as shown in **Figure 5**. The first crack started at around 45 - 55 % of the ultimate load. At 70 - 80 % of peak load, several spread cracks were formed all over the column specimen. The cracks sprouted up on both sides, and the top at the maximum load ultimately caused the concrete cover to spread. **Figure 6** shows the top strengthened RC column element's failure due to GFRP and BFRP wrap rupture with severe core degradation in B2X and G2X. At the bottom corner of the specimen, the un-wrapped concrete cover cracking originated and later spread over the specimen's entire circumference, as shown in B1X and G1X. Subsequently, B2X wraps, break up from the top of the specimen. The small part (fibers) of G2X wraps at the end of the specimens was ruptured. The concrete crack extended from the bottom to top at higher deflection levels and was finally crushed, following the GFRP bi-directional wraps' rupture. The longitudinal bar yielding was observed in the G1X and G2X columns, whereas the longitudinal bar yield in G1X and G2X columns was noticed. The specimen's failure started due to FRP rupture followed by the local debonding of FRP column of damages after peak load in B2X. A concrete crack extended from the top at higher deflection levels and finally ruptured the BFRP bi-directional B2X.

Figure 5 Failure of non-strengthened RC column elements.

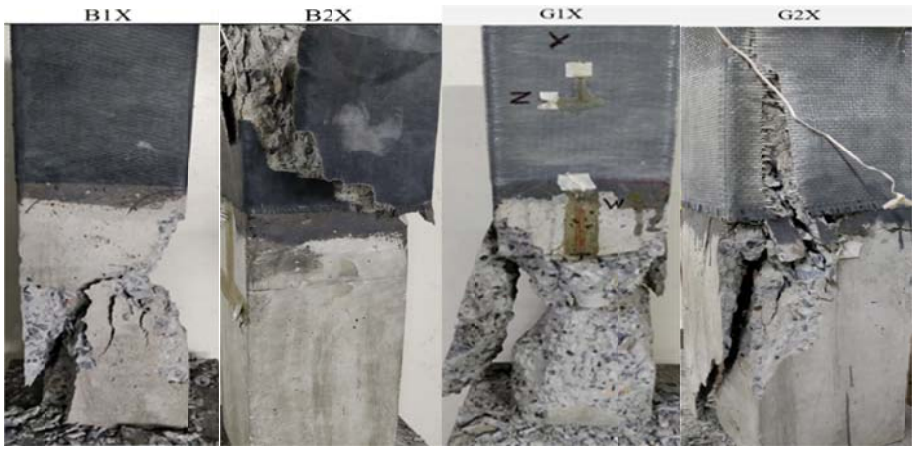

Figure 6 Failure of top-strengthened RC column elements.

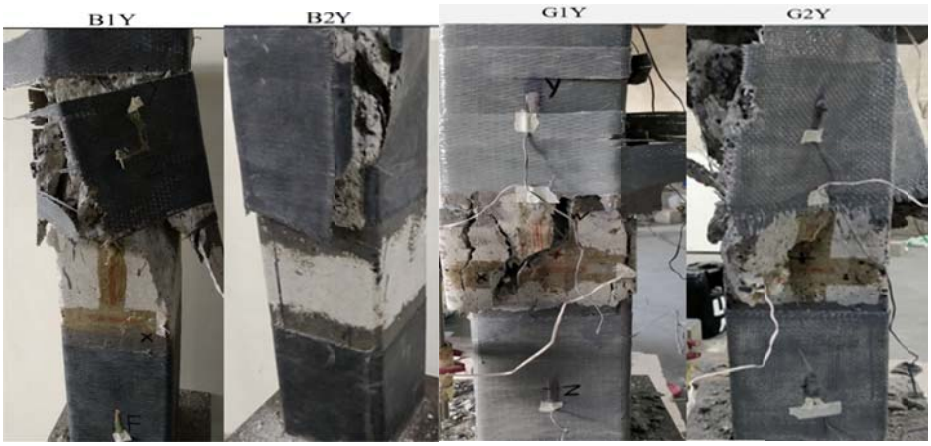

Figure 7 Failure of top-bottom strengthened RC column elements.

The specimen B1Yand B2Y was cracked internally at the yield axial load with snapping sounding. The FRPs were strained due to the cracking of the concrete when the ultimate axial load approached. Later, the top-bottom FRP confinement failure occurred due to the crushing of the concrete cover. An explosive sound was experienced during the failure of the specimen. Under the higher load, the concrete crack extended at mid-height to top and ultimately crushed in the BFRP wraps' rupture at a top side. The top failure in FRP content in the B1Y and B2Y had occurred as shown in **Figure 7**, whereas sudden explosive failure occurred in the B1Y, B2Y column after a slow cracking sound. Due to the high confinement pressure in the top-bottom wrapping, the eruptive failure was observed in which BFRP has detached from the concrete surface.

The specimens G1Y and G2Y were cracked internally at the yield axial load with snapping sounding. The FRPs were strained due to the cracking of the concrete when the ultimate axial load approached. Later, the top-bottom (2h/3) FRP confinement failure occurred due to the crushing of the concrete cover. An explosive sound was experienced during the failure of the specimen. Under the higher load, the concrete crack extended at mid-height to top and ultimately crushed in the GFRP wraps rupture at a top side. The shear failure at the mid-portion of the concrete cover was observed in G1Y, as shown in **Figure 7**. The top failure in FRP content in the G2Y had occurred, as shown in **Figure 7**, whereas sudden explosive failure occurred in the G1Y column after a slow cracking sound. Due to the high confinement pressure in the top-bottom wrapping, the eruptive failure was observed in which FRP has detached from the concrete surface, as shown in **Figure 7**.

Figure 8 Failure of full strengthened RC column elements.

Failure of the entirely confined RC column element occurred due to the crushing of concrete cover and rupture of BFRP wrap at the bottom side in B1Z and topside in B2Z, and the opposite of the overlap wrap zone as shows in **Figure 8**. Similarly, rupture of GFRP wrap at the top side in G1Z and G2Z. The specimens' failure begins with a snap noise due to the concrete's cracking during the test time as seen by visual inspection. GFRP and BFRP ripples formed on the compression side, owing to the concrete surface cracking. Under higher loads, the concrete crushed the inner side and was finally crushed, causing the top of the GFRP and BFRP wrap to crack. During the testing time of the entire confined RC column crushed the concrete after gradual failure at the bottom side in B1Z and topside in B2Z G1Z and G2Z top side. GFRP and BFRP uni-directional material suddenly ruptures failure and explosive way preceded by a typical cracking sound. Following the GFRP and BFRP tensile rupture, the experiment is complete afterward observed that the FRP was detached stick up with its concrete from the column surface. The FRP rupture occurred severely at the corners in full confined column specimens. The difference between the crushing of concrete coverings indicate that the highest lateral confinement pressure was present at the corners.

Load-dispalcement behavior

Experimental results of the axial load-displacement tested specimens are reported in **Table 4**. The Column specimens are divided into 3 different groups for the ease of discussion. The load-displacement behavior of the 3 groups of the RC column [(a) - (b) top-bottom, and (c) full strengthened] including the non-strengthened column is presented in **Figure 9**. In this **Table 4** A_{eff} is the effective column's cross-section (non-strengthen and strengthen); P-ultimate is the ultimate load supported by the column *Δ*P-ultimate = [100×(Pstr-Pnon-str*)*/Pnon-str] represents the increase of load-carrying capacity provided by the strengthened technique. It can be seen that the columns strengthened with conventional GFRP and BFRP techniques (partially and fully strengthened), apart from the case of G1Z and G2Z, have provided a modest increase in terms of strength gain (P-ultimate). The ultimate displacement of Δ L-ultimate = 100×(Lstr -Lnon-str)/Lnon-str represents the displacement control by strengthened square RC columns at P-ultimate.

Table 4 Experimental results of the axial load-displacement tested specimens.

Specimen ID	Aeff (m^2)	P-ultimate (kN)	L-ultimate (m^2)	ΔP-ultimate (%)	ΔL-ultimate (%)
S 1	28900	776.71	9.88	-	-
B1X	28556.64	979.51	11.89	26.11	20.39
B2X	28556.64	859.77	12.67	10.69	28.28
G1X	28556.64	1132.58	13.78	45.82	39.53
G2X	28556.64	967.51	13.72	24.57	38.92
B1Y	28556.64	1043.15	10.97	34.30	11.07
B2Y	28556.64	964.36	11.33	24.16	14.77
G1Y	28556.64	1224.75	11.75	57.68	18.98
G2Y	28556.64	1204.24	10.66	55.68	7.90
B1Z	28556.64	1244.28	13.07	60.20	32.35
B2Z	28556.64	1259.11	12.09	62.11	22.38
G1Z	28556.64	1437.43	14.88	85.07	50.87
G2Z	28556.64	1448.06	12.72	86.43	28.80

In the non-strengthened and strengthened square RC column, the axial load-displacement behavior is demonstrated in **Figure 9**. The column specimens with identical configurations demonstrated an even

more similar response, as shown in **Table 4** and **Figure 9**. Moreover, the displacement control at a given P-ultimate resulted in an increase in the strengthened specimens' ultimate axial load.

The ⊿P-ultimate increase of 26.11, 10.69, 45.82, and 24.57 % were recorded in B1X, B2X, G1X, and G2X strengthened column specimens to S1 respectively. The corresponding increases of the ⊿L-ultimate at P-ultimate of B1X, B2X, G1X, and G2X strengthened column specimens were 20.39, 28.28, 39.53, and 38.92 %, respectively. It was also found that the G1X gives more axial load carrying capacity than other column specimens, as shown in **Figure 4(a)**. Moreover, it was observed that the B2X, G1X, and G2X column were initially less load-carrying compared to S1 and B1X columns as shown in **Figure 9(a)**.

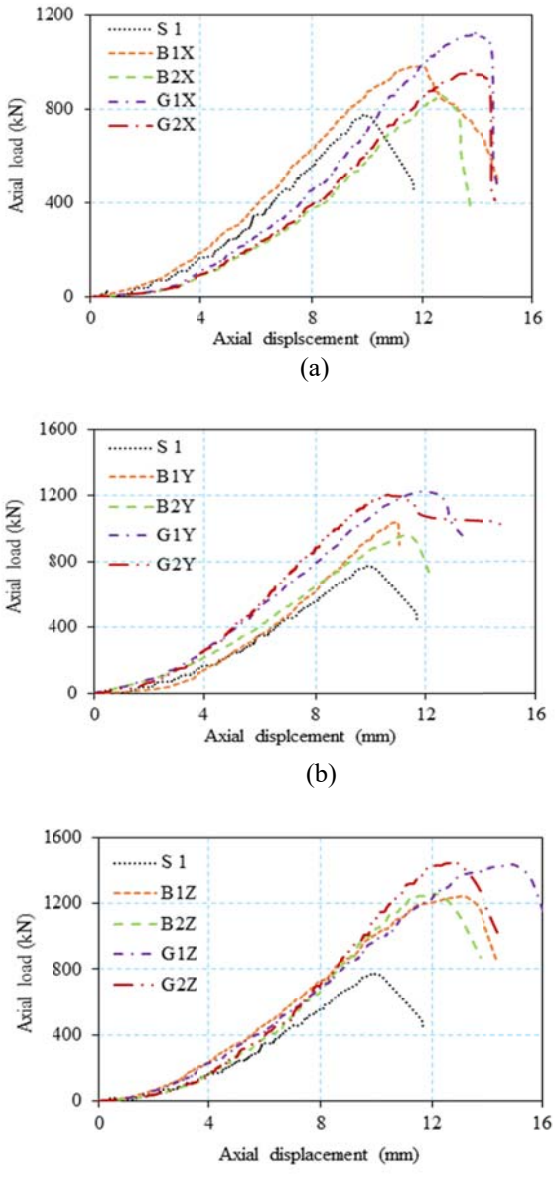

Figure 9 Axial load-displacement of non-strengthed and strengthed square columns: (a) Top strengthened columns, (b) Top-bottom strengthened columns, and (c) Full strengthened columns.

The strengthen column specimens of B1Y, B2Y, G1Y, and G2Y reported compared to S 1, the *Δ*P-ultimate increasing of 34.30, 24.16, 57.68, and 55.68 %, respectively. The corresponding increase of the *Δ*L-ultimate at P-ultimate of B1Y, B2Y, G1Y, and G2Y strengthened column specimens were 11.07, 14.77, 18.98 and 7.90 %, respectively. Moreover, it was observed that the G1Y and G2Y load-carrying capacity was almost identical, and ultimate displacement control capacity was higher in G2Y than in another column specimen, as shown in **Figure 9(b)**.

Compared to the S1, the *Δ*P-ultimate increased by 60.20, 62.11, 85.07 and 86.43 % in the B1Z, B2Z, G1Z, and G2Z strengthened column specimens, respectively. The corresponding increase of the *Δ*L-ultimate at P-ultimate of B1Z, B2Z, G1Z, and G2Z strengthened column specimens were 32.35, 22.38, 50.87 and 28.80 %, respectively. The fully strengthened square RC column increased the ultimate load-carrying capacity and displacement capacity compared to other columns and non-strengthened columns. It was also observed that the B1Z and B2Z columns load-carrying capacity was almost identical, and ultimate displacement control capacity was higher in B2Z than B1Z, as shown in **Figure 4(C)**. G1Z and G2Z columns' ultimate load-carrying capacity performance is almost alike. The ultimate displacement control capacity was higher in G2Z than another column specimen corresponding to the ultimate load-carrying capacity, as shown in **Figure 9(c)**.

Axial stress-strain behavior

The experimental results of the axial stress-strain of the tested specimens are described in **Table 5**. The Column specimens are divided into 3 different groups for the ease of discussion. The axial stress-strain response of 3 groups of the RC column [(a) top, (b) top-bottom, and (c) full strengthened] including non-strengthened column is presented in **Figure 10**. The strain gauge on concrete was placed in the column specimen's mid-height, whereas the strain gauge on FRP wrapping was placed at mid-height of the wrapping. The axial strain of concrete was taken as positive, and the lateral strain of FRP wrapping was taken as negative. In this table, the axial strain of concrete was taken as positive, and the lateral strain of FRP wrapping was taken as negative. The column's axial stress was computed by dividing the axial load to its effective c/s area (σcc=P-ultimate/Aeff), $\Delta\ \sigma cc$ = (100×($\sigma ccStr$-σcc non-str)/σcc non-str) represents the increase of stress carrying capacity provided by the strengthened technique. Moreover, *Δ*εcc = [100× ($\varepsilon ccStr$ - εcc Ref)/ εcc Ref] is the increase of axial strain at P-ultimate and FRP efficiency ratio and *Δ*εf max = εf max / εf (the ratio between the average ultimate FRP hoop strains and the FRP rupture strain obtained from the coupon tests (εf) for all test specimens. The testing of the specimen ended at the point of FRP rupture unless it is specified.

Table 5 Experimental results of the axial stress-strain of tested specimens.

Specimen ID	σcc (MPa)	εcc (%)	εf max (%)	Δσcc (%)	Δεcc (%)	Δεf max (%)
S 1	26.88	1.83	-	-	-	-
B1X	34.30	2.65	0.68	27.60	45.1	26.2
B2X	30.11	2.35	1.09	12.02	28.5	47.4
G1X	39.66	2.84	1.67	47.54	55.4	72.6
G2X	33.88	2.96	1.69	26.04	61.6	86.2
B1Y	36.53	2.10	1.73	35.90	14.6	66.5
B2Y	33.77	1.84	1.42	25.63	0.6	61.7
G1Y	42.89	2.68	2.20	59.56	46.6	95.7
G2Y	42.17	3.20	2.38	56.88	74.9	121.4
B1Z	43.57	2.62	2.06	62.09	43.4	79.2
B2Z	44.09	2.42	1.84	64.03	32.5	80.0
G1Z	50.34	3.60	1.56	87.28	98.5	67.8
G2Z	50.71	4.83	3.72	88.65	164.1	189.8

The axial stress-strain relations of FRP-strengthened column specimens are shown in **Figure 10**. **Figure 10** indicates that increase in σcc contributed to a significant increase in the ultimate axial strain. Compared to the axial strain of FRP-strengthened column specimens, the lower increase in the corresponding lateral strain. **Figure 10** also demonstrates that the strengthened column specimens in axial strain initially increase at a typically linear rate with the axial load applied. However, after reaching the ultimate load, this axial strain starts to decrease significantly and quickly. As shown in **Figure 10**, the axial strain in the column specimens increased and then decreased, while the increase in the concrete's axial strain is due to the strengthening's contribution. It is also significantly noted that the load applied first on column concrete core and then transferred to the strengthened material after it ruptured concrete.

B1X, B2X, G1X and G2X column specimens respectively show an ultimate axial strain increase of 45, 28.5, 55.4 and 61.6 % and corresponding ultimate lateral strain ratio increase by 26.2, 47.4, 72.6 and 86.2 % and with an enhancement of an ultimate axial stress by 27.6, 12.02, 47.54 and 26.04 %, respectively. **Figure 10(a)** shows that the ultimate strain in the G2X column specimens was observed higher than axial strain and lateral strains than the S 1, B1X, B2X, and G1X. It was also noted that the B1X in lateral strain had declined gradually, and B2X, G1X, and G2X in lateral strain gas suddenly declined. The top strengthens column in the stress-strain behavior initially elastic phase of the BFRP bi-directional peak performed well.

The strengthen columns specimens of B1Y, B2Y, G1Y, and G2Y, reported as compared to S1, ultimate axial strain increase by 14.6, 0.6, 46.6 and 74.9 % and corresponding ultimate lateral strain ratio increase by 66.5, 61.7, 95.7 and 121.4 % and with an enhance ultimate axial stress 35.9, 25.63, 59.63 and 56.88 %, respectively. The square RC columns top-bottom strengthened by BFRP and GFRP uni and bi-directional show resembling behavior against the axial and lateral strains in the elastic stage like the top strengthen column as shown in **Figure 10(b)**. The top-bottom strengthen columns axial and lateral strains slightly increase and lead to failure severely delayed.

Compared to S1, the strengthened column specimens of B1Z, B2Z, G1Z and G2Z reported a 43.4, 32.5, 98.5 and 164.1 % ultimate axial strain increase and a corresponding 79.2, 80, 67.8 and 189.8 % ultimate lateral strain ratio increase and a 62.09, 64.03,87.28 and 88.65 % of ultimate axial stress increase. The stress-strain behavior on BFRP and GFRP wrapping in full strengthened column specimen was observed almost the same as concrete strain behavior shown in **Figure 10(c)**. It is because of the total FRP confinement on the concrete surface. **Figure 5(c)** shows the behavior of axial and lateral strains elastic to plastic stage gradually travel. The full strengthened column so that the load-carrying capacity increases and the failure occurs with significant delay. From an overall observation, the poor behavior can be observed in BFRP bidirectional in the top and top-bottom specimens.

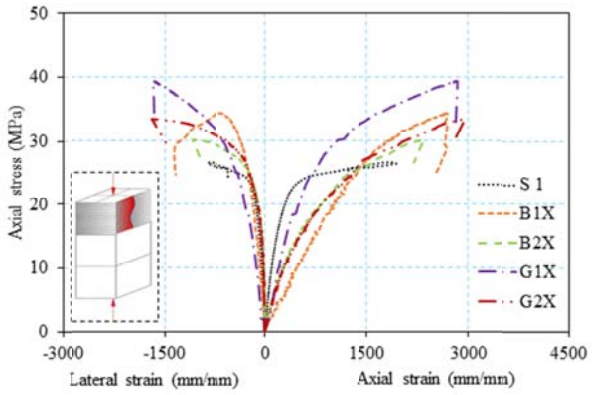

(a)

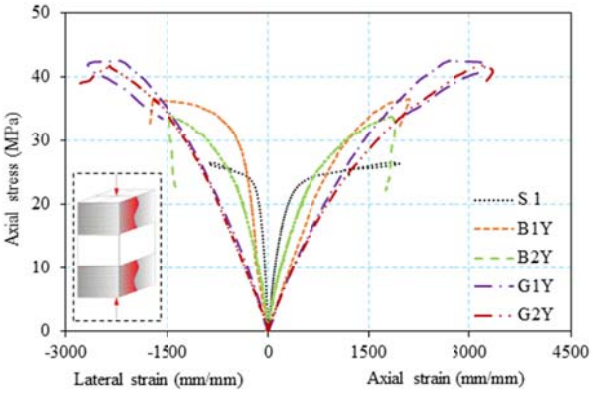

(b)

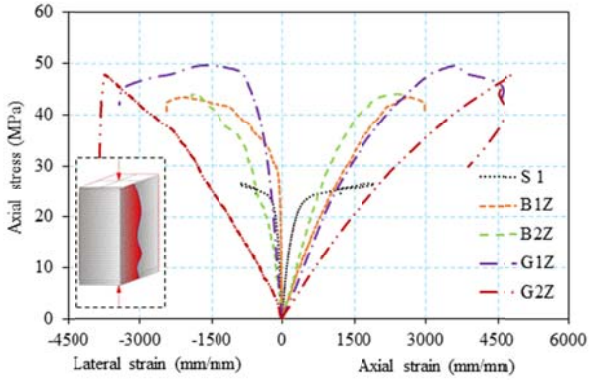

(c)

Figure 10 Axial stress-strain of non-strengthed and strengthed square columns: (**a**) Top strengthened columns, (b) Top-bottom strengthened columns, and (c) Full strengthened columns.

Comparison of experimental stress with a different model

The partially and fully FRP-confined RC column design has been given in the CNR-DT 200 R1 [22]. Adequate confinement pressure and vertical efficiency coefficient are recommended in code for partially confined FRP RC column. To ensure the accuracy of the design criteria for FRP-confined concrete, it mainly depends on the restraint model. To this end, the existing CNR-DT 200 R1 [22] restriction model has been briefly described in the following sections. Some codes used the theoretical model of Lam and Teng [23]. The experimental data were compared with the above 2 models to check the precision and reliability.

CNR-DT 200 R1 model of FRP-confined concrete

The ultimate axial stress of the RC column is in CNR-DT 200 R1 [22], provided as follows:

$$\frac{f'_{cc}}{f'_{co}} = 1 + 2.6\left(\frac{f_{l,eff}}{f'_{co}}\right)^{\frac{2}{3}} \quad (1)$$

Lam and Teng's analytical model

Numerous supplementary codes propose different strengthened methods for FRP-confined concrete. Previously, it was observed that some codes had less availability for design requirements of partially FRP-constrained concrete. In this study of Lam and Teng's model, some FRP-constrained concrete's vertical efficiency coefficients are correlated to see if the model can evaluate the ultimate axial stress. In Lam and Teng's model, the ultimate axial stress was estimated as follows:

$$\frac{f'_{cc}}{f'_{co}} = 1 + 3.3\,\frac{f_l}{f'_{co}} \quad (2)$$

where f'_{cc} = Ultimate axial stresses, f'_{co} = The unconfined concrete strength, f_l = adequate confining pressure of FRP.

In partially FRP-constrained concrete, the vertical efficiency coefficient [22] is used with the Lam and Teng model [23]. The test results are closely related to the Lam and Teng models [23].

A detailed analysis of determining the axial stress, partially and fully strengthened axially loaded square and RC columns using Lam and Teng model and CNR-DT-R1-2013[22] guidelines is provided. The ultimate axial stress shows the carrying capacity comparison of experimental and theoretical results, as shown in **Figure 11**. The strengthened square columns' ultimate axial stress matches the Lam and Teng model [23] and CNR-DT-R1-2013 [22] results. **Figure 11** the results show that the CNR-DT-R1 model is more reliable than Lam & Tang and provides reasonable and precise calculations for the ultimate axial stress of partially and fully wrapped RC columns.

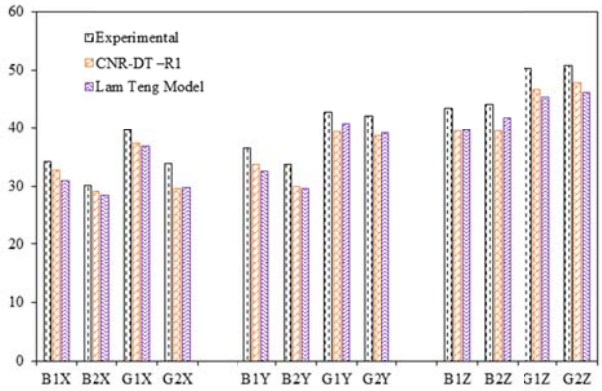

Figure 11 Comparisons of axial stress for strengthened columns.

Conclusions

This paper presents the numerical and experimental test results of 13 different types of columns. The present study predicted the experimental stresses with a different model like CNR-DT-R1 and Lam and Teng. The following conclusions can be drawn:

Significant increases in the axial load and axial displacement capacity are obtained for FRP partially and fully wrapped column specimens compared to non-strengthened. The FRP entirely wrapped columns, and FRP partially wrapped columns are mostly failed due to the rupture of FRP. Moreover, G2X and G1Y columns were a sheer failure. Partial top strengthened of square RC column led to increasing displacement than a controlled column in BFRP. GFRP wraps about 20.39 and 39.53 % higher in uni-directional and about 28.38 and 38.92 % higher in bi-directional respectively. Moreover, it was also found that the G1X gives more axial load carrying capacity than other column specimens.

The partially top-bottom strengthened of RC square column by BFRP and GFRP was 11.07 and 18.98 % higher in uni-directional and 14.77 and 7.98 % higher in bi-directional respectively. Moreover, it was observed that the load-carrying capacity increased, and ultimate displacement control capacity was higher in the partially top-bottom strengthened techniques as compared to the partially top strengthened technique. The fully strengthened square RC column increased the ultimate load-carrying capacity and displacement capacity compared to the top and top-bottom strengthen columns and non-strengthened columns. The entire strengthened square RC column than the controlled column in BFRP and GFRP wraps was recorded about 32.35 and 50.87 % in uni-directional wrapping and 22.38 and 28.80 % in bidirectional wrapping respectively. Moreover, the ultimate displacement control capacity was higher than another column specimen corresponding to the ultimate load-carrying capacity.

The axial stress-strain curve of the partial FRP strengthened column includes 2 stages. Increasing the FRP strengthened usually results in ultimate axial stress strain. In general, the slope and stiffness of the second phase of the stress-strain curve increase with FRP. It was also noted that the B1X in lateral strain declined gradually, and B2X, G1X, and G2X in lateral strain gas suddenly declined. The top strengthens column in the stress-strain behaviour initially elastic phase of the BFRP bi-directional peak performed well. The top-bottom strengthened column's axial and lateral strains slightly increase and lead to the failure severely delayed. The design code CNR-DT-200 R1 and Lam and Teng model can provide accurate predictions for the ultimate axial stress of a partially and fully FRP confined RC column. The strength formula of CNR-DT200R1 and the ultimate axial stress obtained by the experiment are

approximately equal. Similarly, the Lam and Tang model results revolve around the ultimate axial stress of partially and fully FRP-restrained RC columns. Strengthened FRP composite material in BFRP had an ultimate load-carrying capacity near a GFRP in full strengthened columns. This result is exciting from the cost-efficiency point of view.

References

[1] H Saadatmanesh, MR Ehsani and MW Li. Strength and ductility of concrete columns externally reinforced with fiber composite straps. *ACI Struct. J*. 1994; **91**, 434-47.

[2] S Rocca, N Galati and A Nanni, Interaction diagram methodology for design of FRP-confined reinforced concrete columns. *Construct. Build. Mater.* 2009; **23**, 1508-20.

[3] MNS Hadi. Behaviour of FRP strengthened concrete columns under eccentric compression loading. *Compos. Struct.* 2007; **77**, 92-6.

[4] MNS Hadi. Comparative study of eccentrically loaded FRP wrapped columns. *Compos. Struct.* 2006; **74**, 127-35.

[5] PF Marques and C Chastre. Performance analysis of load-strain models for circular columns confined with FRP composites. *Compos. Struct*. 2012; **94**, 3115-31.

[6] IAEM Shehata, LAV Carneiro and LCD Shehata. Strength of short concrete columns confined with CFRP sheets. *Mater. Struct*. 2002; **35**, 50-8.

[7] K Galal, A Arafa and A Ghobarah. Retrofit of RC square short columns. *Eng. Struct*. 2005; **27**, 801-13.

[8] G Karam and M Tabbara. Confinement effectiveness in rectangular concrete columns with fiber reinforced polymer wraps. *J. Compos. Construct.* 2005; **9**, 388-96.

[9] MH Harajli. Axial stress-strain relationship for FRP confined circular and rectangular concrete columns. *Cement Concr. Compos.* 2006; **28**, 938-48.

[10] HJ Lin and CI Liao. Compressive strength of reinforced concrete column confined by composite material. *Compos. Struct.* 2004; **65**, 239-50.

[11] YC Wang and K Hsu. Design of FRP-wrapped reinforced concrete columns for enhancing axial load carrying capacity. *Compos. Struct.* 2008; **82**, 132-9.

[12] MNS Hadi and IBR Widiarsa. Axial and flexural performance of square RC columns wrapped with CFRP under eccentric loading. *J. Compos. Construct.* 2012; **16**, 640-9.

[13] V Yazici and MN Hadi. Axial load-bending moment diagrams of carbon FRP wrapped hollow core reinforced concrete columns. *J. Compos. Construct.* 2009; **13**, 262-8.

[14] A Saljoughian and D Mostofinejad. Axial-flexural interaction in square RC columns confined by intermittent CFRP wraps. *Compos. B Eng.* 2016; **89**, 85-95.

[15] A Saljoughian and D Mostofinejad. Corner strip-batten technique for FRP-confinement of square RC columns under eccentric loading. *J. Compos. Construct.* 2016; **20**, 04015077.

[16] K Soudki and T Alkhrdaji. Guide for the design and construction of externally bonded FRP systems for strengthening concrete structures (ACI 440.2R-02). *In*: Proceedings of the Structures Congress, New York, United States. 2005, p. 1-8.

[17] AD Mai, MN Sheikh and MNS Hadi. Investigation on the behaviour of partial wrapping in comparison with full wrapping of square RC columns under different loading conditions. *Construct. Build. Mater.* 2018; **168**, 153-68.

[18] G Campione, L La Mendola, A Monaco, A Valenza and V Fiore. Behavior in compression of concrete cylinders externally wrapped with basalt fibers. *Compos. B Eng.* 2015; **69**, 578-86.

[19] MFM Fahmy and Z Wu. Evaluating and proposing models of circular concrete columns confined with different FRP composites. *Compos. B Eng*. 2010; **41**, 199-213.

[20] M Di Ludovico, A Prota and G Manfredi. Structural upgrade using basalt fibers for concrete confinement. *J. Compos. Construct.* 2010; **14**, 541-52.

[21] V Fiore, G Di Bella and A Valenza. Glass-basalt/epoxy hybrid composites for marine applications. *Mater. Des.* 2011; **32**, 2091-9.

[22] R Realfonzo and AAVV. *Guide for the design and construction of externally bonded frp systems for strengthening existing structures.* Italian National Research Council, Rome, Italy, 2006.

[23] L Lam and JG Teng. Design-oriented stress-strain model for FRP-confined concrete. *Construct. Build. Mater*. 2003; **17**, 471-89.

[24] Indian Standard. *Plain and reinforced concrete*. Bureau of Indian Standards, New Dehli, India, 2000, p. 1-114.

[25] Indian Standard. *High strength deformed steel bars and wires for concrete reinforcement-*

specification. Bureau of Indian standards, New Delhi, India, 2008, p. 1-12.
[26] Indian Standard. *Guidelines for concrete mix design proportioning*. Bureau of Indian Standards, New Delhi, India, 2009, p. 1-21.
[27] American Society for Testing and Materials. *Annual book of ASTM standards*. American Society for Testing and Materials, Pennsylvania, 2014, p. 1-13.